Colloidal Pumping: Evidence for the Coagulation Process Using Natural Colloids Tagged with 203Hg

3 AUTHORS, INCLUDING:

Peter H. Santschi

Texas A&M University - Galveston

337 PUBLICATIONS **12,625** CITATIONS

SEE PROFILE

Gary A. Gill

Pacific Northwest National Laboratory

87 PUBLICATIONS **4,009** CITATIONS

SEE PROFILE

Colloidal Pumping: Evidence for the Coagulation Process Using Natural Colloids Tagged with 203Hg

MARY C. STORDAL,*
PETER H. SANTSCHI, AND
GARY A. GILL

Department of Oceanography, Texas A&M University at Galveston, 5007 Avenue U, Galveston, Texas 77551

Colloids isolated from waters of the Trinity River (Texas) were tagged with high specific activity mercury (203Hg) and re-equilibrated with ultrafiltered water and particles. The transfer of radioisotopic Hg from the colloidal pool to the particulate pool was monitored over a 5-day period. The experiment was repeated with a range of particle concentrations from 10 to 82 mg/L and at salinities of 13.6 and 24.5. Partitioning of 203Hg to particles and colloids during the radiotracer experiments was comparable or slightly higher than that observed for stable Hg in Galveston Bay. In all cases, 203Hg was transferred from the colloidal pool (1 kDa−0.4 μm), consisting mostly of macromolecular organic matter, to the particulate pool (>0.4 μm), indicating that colloids serve as an intermediary in the transfer and removal of Hg and perhaps other trace metals in natural systems. The rate of transfer was determined by applying an irreversible kinetic model to the data. The transfer appeared to occur by two processes, a fast (<1 h) initial process and a slower process that occurred over days. Both processes were proportional to particle concentration (C_p) expressed as a power function $C_p^{0.3}$, suggesting that Brownian coagulation is the mechanism responsible for slow transfer. Measured rates were consistent with coagulation rates calculated from coagulation theory.

Introduction

The fate of trace metals in the aquatic environment has been postulated to be primarily controlled by complexation with ligands in solution and on particle surfaces (*1−4*). These types of reactions are generally very rapid and would suggest that highly particle reactive species such as Th(IV) and Hg(II) would be strongly bound to particle surfaces and, as such, rapidly removed from the water column. The concentrations in the "dissolved phase", defined as the concentration in water that has passed a 0.45-μm filter, is often assumed to reflect mostly inorganic solution species, with organic species being unimportant (*5*). Measurements of trace metals and organic matter in this fraction separated

according to molecular weight have however yielded significant concentrations of trace elements (including Hg) bound to organic matter of high molecular weight, suggesting that current models are not adequate (*6−8*). Microparticles and macromolecules that pass through a 0.45-μm filter, herein defined as colloids, have been suggested as an important link between the truly dissolved and particulate phases. Coagulation of colloids has been postulated as the process responsible for slow sorption kinetics (*9−11*).

Honeyman and Santschi (*11*) applied the coagulation theory to model particle-reactive Th(IV) removal from the ocean using the formulation of Farley and Morel (*12*) to incorporate colloids as an intermediary in particle removal processes; they refer to this coagulation process as "colloidal pumping". In this model, particle-reactive species such as dissolved Th(IV) are rapidly and irreversibly adsorbed onto colloidal particles, which in turn coagulate slowly into the particulate pool. Similar processes have also been postulated, albeit less quantitatively, by Li et al. (*9, 13*), Nyffeler et al. (*10*), Santschi et al. (*14*), and Niven and Moore (*15*). Slow sorption kinetics have important implications to the fate and transport of trace elements in environments, such as estuaries, where particle residence times are short.

We report here the results from investigations into the importance of colloidal pumping on Hg(II) cycling in estuarine waters. A series of experiments were conducted using water, particles, and colloids from Galveston Bay and Trinity River, the major freshwater inflow to Galveston Bay. Colloids isolated from Trinity River water were tagged using high specific activity 203Hg at near ambient concentrations. By using equilibrated, 203Hg-tagged colloids, the transfer of colloidal Hg(II) to the particulate pool could then be examined as a coagulation process separate from adsorption.

Materials and Methods

Sample Collection. A seawater sample (salinity = 27.5) was collected from Rollover Pass on Bolivar Peninsula that connects East Bay (part of the Galveston Bay system) with the Gulf of Mexico. A freshwater sample was collected from the Trinity River about 2 mi upriver from the mouth, which drains into upper Galveston Bay. Samples were collected using precleaned Teflon tubing and a peristaltic pump and were filtered through a 0.45-μm MSI in-line cartridge that had been rigorously precleaned (*6, 8*). A 20-L Teflon "bag-in-a-bottle" (Berghof) was used to collect the sample for ultrafiltration. Samples for total and filter-passing Hg (<0.45 μm) were collected in precleaned Teflon bottles. Samples for suspended particulate matter (SPM) were also collected. An unfiltered freshwater sample from the Trintiy River was collected in a 20-L bottle as a source of particles for the experiments described below.

Ultrafiltration Procedures. The samples were immediately ultrafiltered after return to the lab (within 1 h) using an Amicon spiral-wound ultrafiltration cartridge (S10N1) with a nominal molecular mass cutoff of 1 kDa (*6−8*). The ultrafiltration process took about 4 h with a final concentration factor of approximately 18. The concentrated retentate containing the colloids from the freshwater sample was stored in a Teflon bottle. The

permeate (or filtrate) from both the seawater and freshwater samples was collected in 2-L Teflon bottles for use in the experiments. Both retentate and permeate samples were analyzed for Hg (16).

Preparation of [203]Hg-Tagged Colloids. A 50-mL aliquot of the colloids (concentrated retentate from the freshwater sample) was placed in a dialysis bag (Spectra/Por membrane, Spectrum) with a nominal molecular mass cutoff of 1 kDa and immersed in deionized water. For most of the experiments, the colloids were aliquoted spiked with [203]Hg immediately after separation by ultrafiltration, thus using the freshest possible colloidal material. The colloids were then equilibrated for at least 48 h, while the outer water was changed at least twice. The [203]Hg spike had a specific activity of 37 mCi/mg, allowing for spiking concentrations near ambient levels, i.e., not more than 4 ng/L was spiked into the diafiltration bags with the colloids as compared to 1−4 ng/L ambient Hg concentrations (6).

Concentrated Particle Solution. A concentrated particle solution was generated by allowing 20 L of unfiltered Trinity River water to settle for 60 h, the overlying water was decanted, and the remaining water plus particles (~1 L) were transferred to a 1-L Teflon bottle. The settling time was long enough to allow particles >1 μm to settle according to Stoke's law. The particle solution was examined through a microscope to verify that a complete spectrum of particles was present. The concentration factor of this solution was approximately 20, so the addition of 50 mL to 1 L was expected to yield a particle concentration similar to the original source water. The suspended load was checked at the end of each experiment to verify particle concentration.

Laboratory Experiments. One-liter Teflon bottles were filled with filtrate (<1 kDa) water either from freshwater, saltwater, or a mixture. Varying amounts of the concentrated particle solution (>1 μm) were added, and the solutions were allowed to equilibrate with constant stirring at ~100 rpm for 2 h. The spiked colloids were added, and a 50-mL subsample was immediately removed and filtered through a Nuclepore 0.45-μm filter. The filtrate was then transferred to an Amicon stirred cell ultrafiltration unit (Model 8200) containing a 1-kDa cellulose acetate filter and ultrafiltered until 10−15 mL remained in the cell (~45 min). A 20-mL aliquot of the water with particles (total water) was also collected and placed in a scintillation vial for γ-counting. The 0.45-μm filter, retentate from the stirred cell (0.45 mm−1 kDa), and filtrate from the stirred cell (<1 kDa) were all collected in 20-mL scintillation vials for γ-counting. Additional samples were taken at 5, 10, 15, 30, and 60 min and 24, 72, and 120 h after adding the colloids. At the end of each experiment, pH, salinity, SPM, and total Hg concentration were measured. All experiments were conducted at room temperature (24 °C) under ambient light. A wash of the Teflon bottles was also conducted with 6 N HCl to check for wall adsorption of Hg at the end of the experiment. The results indicated that less than 4% of the original amount of [203]Hg spiked was lost to the walls.

γ-energies (279 keV) were counted in a solid scintillation detector using a well-type NaI crystal (5 1/4 in., Harshaw Chemical) interfaced to a multi-channel analyzer (NaI-plus board, Canberra) installed in an IBM-compatible PC (17). The samples were counted until at least 1000 net counts were accumulated, yielding 3% standard deviation from counting statistics.

Two experiments were conducted without the particles. The tagged colloids were added to separate containers filled with ultrafiltered freshwater and seawater and subsampled at 1, 2, 24, 72, and 96 h. Results from these experiments indicated that the colloids had coagulated (60% in seawater and 50% in freshwater) into filterable particles during the tagging process. This observation was confirmed in separate experiments in which [203]Hg was added to untagged colloids and the adsorption of [203]Hg was monitored over time.

Colloid Composition. The observation that the colloids coagulated over time until some steady state was obtained was used to estimate the mass of the colloidal material. This parameter is necessary in order to model the coagulation of colloids. The mass concentration of the colloids was estimated by measuring the mass of the coagulated colloids separated on preweighed 0.45-μm Nuclepore filter. The organic carbon content of the colloid-containing solution was then measured before and after filtering. We found that about 10% of the colloidal matter had coagulated into the particulate fraction. The difference in organic carbon was used to estimate a mass to carbon ratio in the coagulating colloidal pool of 2.97. This value is broadly similar to the value of 2.0−2.5 calculated from values given in Buffle (18). Analysis of the composition of the colloids for organic carbon, iron, manganese, and aluminum indicated that at least 98% of the colloidal mass is due to organic carbon assuming a mass to carbon ratio of 2.5 based on a chemical formula of CH_2O.

Mass Balance Calculations. The fraction of [203]Hg in the filtered (>0.45 μm), colloidal (1 kDa−0.45 μm), and dissolved (<1 kDa) phases was calculated by taking the activity (cpm/mL) for each fraction and dividing by the sum of the three fractions. A mass balance check was performed for each subsample by adding together the activity for each fraction [i.e., particulate (>0.45 μm), retentate (1 kDa−0.45 μm, corrected for low molecular weight fraction), and filtrate (<1 kDa)] and dividing by the activity of a total aliquot taken at each time. Since strongly sorbing ionic forms of Hg were not present in the experimental vessels, sorption of Hg(II) to filters is expected to be minimal. Mass balances ranged from 70 to 120% with the majority between 80 and 100% reflecting counting errors of 3% for each fraction, moderate but irreversible sorption losses of colloidal forms of Hg(II) during the transfer of the solutions.

Results and Discussion

SPM, total Hg, and pH determinations for the freshwater and seawater samples collected and for each experiment are given in Table 1. The SPM concentration in the collected samples was 22 mg/L in the Trinity River and 29 mg/L in the sample from Rollover Pass. The particle concentrations in the experiments closely matched these values except where intentionally varied. The total Hg in the experiments was within the range observed previously in Texas estuaries (6). The pH varied from the collection pH of 7.4 to approximately pH 8.2 in each of the experiments. The reason for this shift in pH is unknown but seems to be linked to the equilibration of particles and water, which must have altered the buffer capacity of the systems.

Freshwater Sample. The first experiment was intended to explore the coagulation rates of colloidal [203]Hg in freshwater systems by recreating the natural river system (SPM = 22 mg/L; colloidal organic carbon = 2.5 mg/L) but with tagged colloids. Initially, 58% of the [203]Hg was collected on the filter (Figure 1). This high initial value was due

TABLE 1
Summary of Salinity, pH, Suspended Particulate Matter (SPM), and Total Hg Concentrations for Different Experiments and Samples Collected from Galveston Bay

experiment	salinity	pH	SPM (mg L^{-1})	total Hg (ng L^{-1})
particles	0.1	8.4	27	3
particles × 1/2	0.1	8.3	10	2.5
particles × 2	0.1	8.7	42	3.2
particles × 4	0.1	8.4	82	4.2
seawater	24.4	8.1	34	2.7
intermediate salinity	13.6	8.1	30	2.6
seawater, no particles	25.7	7.9		2.5
freshwater, no particles	0.1	8.3		2.5
sample				
Trinity River 10-28-95	0.1	7.4	22	0.96
Rollover Pass 10-7-95	27.5		29	1.6
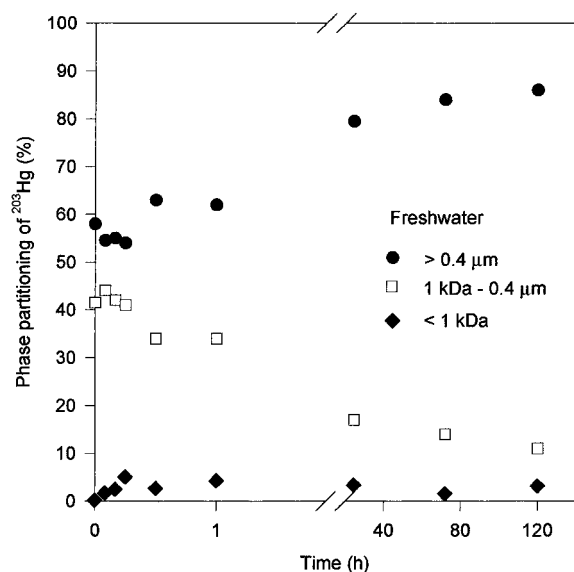
FIGURE 1. Percentages of particulate (>0.4 μm), colloidal (1 kDa–0.4 μm) and truly dissolved (<1 kDa) ^{203}Hg versus time (h) for the Trinity River water at a particle concentration of 27 mg/L.

FIGURE 2. Changes in the percentage of ^{203}Hg in particulate (>0.4 μm) form over time (h) for the experiments with Trinity River water and ^{203}Hg tagged colloids with and without particles.

FIGURE 3. Changes in the percentage of ^{203}Hg in particulate (>0.4 μm) form over time (h) in Trinity River water for four different particle concentrations.

primarily to coagulation of the colloids during the dialysis process. A separate experiment without particles was conducted to examine coagulation alone. Approximately 45% of the colloids were collected on the filter, which remained constant with time (Figure 2). However, after 72 h, almost 85% of the Hg was associated with the particulate fraction when larger particles were present (Figures 1 and 2). Concurrently, the colloidal fraction of ^{203}Hg also decreased from 42% to 11% (Figure 1). These experiments clearly demonstrate that the increase in the particulate fraction is largely due to the combination of coagulation of colloidal ^{203}Hg within the colloidal pool and interaction of the colloids with particles.

Particle Concentration Variations. Particles were added to ultrafiltered freshwater at concentrations of 10, 27, 42, and 82 mg/L to evaluate the effects of particle concentration on coagulation rates (Figure 3). As can be seen, the initial values ($t = 0$) increased with increasing particle concentration. The 10 mg/L experiment reached equilibrium with about 87% of ^{203}Hg in the particulate fraction while in the 82 mg/L experiment, almost 95% of the $^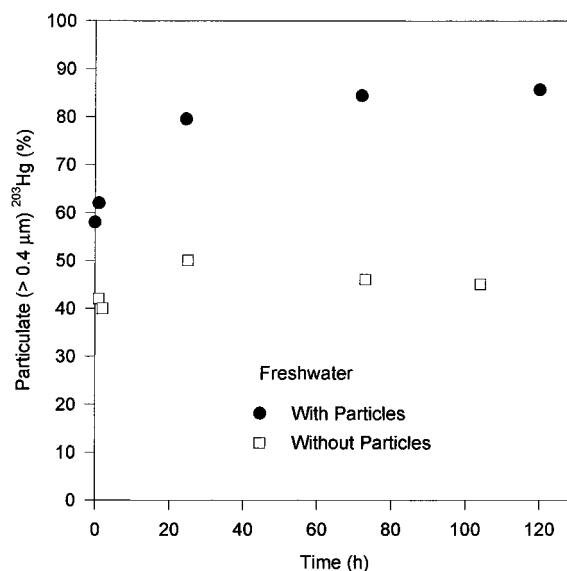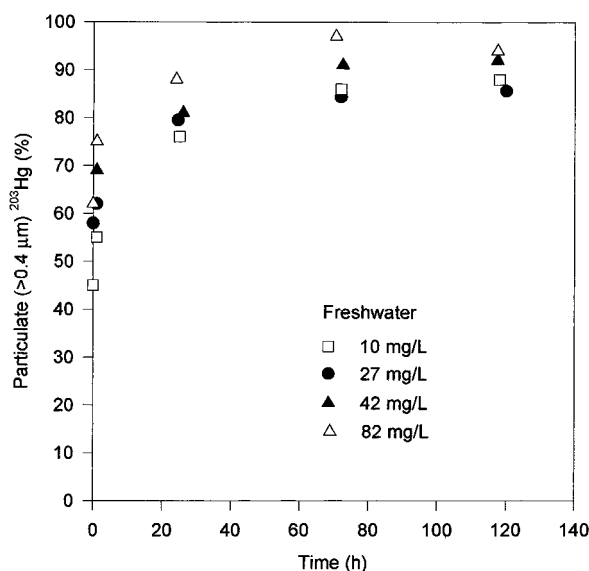{203}$Hg was in the particulate fraction. Furthermore, at higher particle concentrations, the colloidal ^{203}Hg was transferred faster to the particulate fraction, with the 82 mg/L river water showing 75% of the added ^{203}Hg in the particulate fraction within the first hour.

Salinity Variations. The effects of varying salinity on coagulation rates was evaluated at two salinites, 13.6 and 24.4. Very rapid coagulation (in the first hour) was observed for ^{203}Hg in seawater, while freshwater had the slowest coagulation kinetics (Figure 4). In all three experiments, ^{203}Hg was 86–90% particulate at the end of the 5-day experiment. An additional experiment without particles indicated that the ^{203}Hg-tagged colloids coagulated within the first minute to 40% particulate in the freshwater (Figure 2) and 55% particulate in seawater (Figure 5). Without particles, the colloidal ^{203}Hg reached an equilibrium distribution (within 1 h) between 60 and 65% particulate, lower than the 90% in the experiment with particles.

The addition of ^{203}Hg-tagged colloids to ^{203}Hg free ultrafiltered seawater could have resulted in desorption by
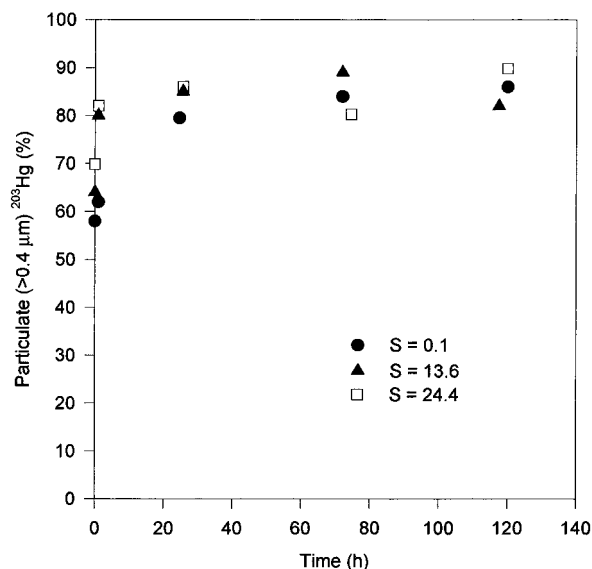
FIGURE 4. Changes in the percentage of [203]Hg in particulate (>0.4 μm) form over time (h) for three different salinities.
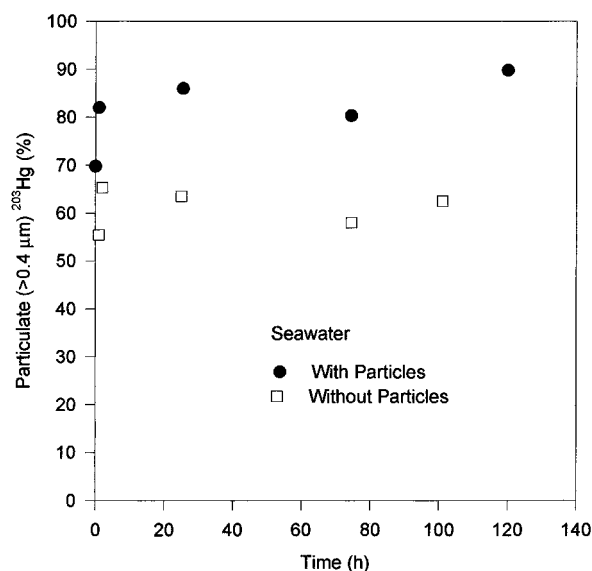

FIGURE 5. Changes in the percentage of [203]Hg in particulate (>0.4 μm) form over time (h) for the mixing of seawater and [203]Hg tagged colloids with (at 34 mg/L) and without particles.

the formation of stronger chloride complexes or exchange with Ca^{2+} (*19*). However, we did not observe significant amounts (<5%) of [203]Hg in the ultrafiltered solution (<1 kDa), indicating that desorption or exchange is not a significant process for elements already bound to colloids.

Particle−Water Partition Coefficients. The particle−water partition coefficient (K_d) represents the equilibrium distribution of a given element between the particulate and dissolved phase. Historically, "dissolved" is operationally defined by filtration with 0.2−0.45-μm filters, which would include the colloid fraction. Through the use of ultrafiltration, we are able to separate the colloidal fraction (defined as 1 kDa−0.45 mm) from the truly dissolved phase (<1 kDa). It is then possible to compare different partition coefficients defined as follows: calculated with the colloidal fraction included in the dissolved phase (K_d); calculated with the colloidal fraction included in the total particulate (K_{p+c}) phase; calculated excluding the colloidal fraction completely (K_p); and calculated between the colloidal and truly dissolved fractions (K_c) (see Table 2 legend for exact definitions). Distribution coefficients, calculated for the six experiments at varying particle concentrations and salinities, are given in Table 2. Also, average partition coefficients of stable Hg at ambient concentrations for samples collected from Galveston Bay in October 1994 (*6*) are presented for comparison (Table 2). Even though, in all cases, the K values are somewhat higher for the radiotracer experiments than for samples collected from Trinity River and Galveston Bay, the relative sequence of $K_d < K_p \approx K_c$ is similar in both cases. Differences in experimental conditions, particle types, and Hg sources may have caused the slight offset between laboratory and field data sets.

Modeling Coagulation Rates of Colloidal Hg. Previous studies of metal ion adsorption kinetics have included colloids in the dissolved phase (*9, 10, 20*). Jannasch et al. (*20*) observed as many as three processes occurring before systems consisting of natural particles and seawater reached equilibrium for different metals. Our experimental design eliminated direct adsorption of the free Hg(II) ion onto particle surfaces. The processes we observed should therefore be either coagulation of the colloidal particles into and onto filterable particles and/or ion exchange between the different fractions. Concentration changes of [203]Hg with time in the different fractions can be treated using models of sorption kinetics similarly to Nyffeler et al. (*10*) and Jannasch et al. (*20*). Alternatively, data can be compared with model predictions using coagulation theory as applied to marine systems by Honeyman and Santschi (*11*) using the coagulation formulation of Farley and Morel (*12*).

Assuming a first-order irreversible reaction model, the rate of transfer of [203]Hg from the colloidal pool to the particulate pool can be described by

TABLE 2

Particle−Water Partition Coefficients for Experiments Using [203]Hg-Tagged Colloids and Estaurine Samples from Galveston Bay[a]

experiment	log C_p (kg L^{-1})	log K_d (L kg^{-1})	log K_p (L kg^{-1})	log K_c (L kg^{-1})	log K_{p+c} (L kg^{-1})
particles	−4.57	5.4	6.0	6.0	5.7
particles × 1/2	−5.00	5.4	6.4	6.4	6.1
particles × 2	−4.38	5.7	6.2	6.2	5.4
particles × 4	−4.09	5.7	6.4	6.4	5.8
seawater	−4.47	5.5	5.9	5.8	5.2
intermediate salinity	−4.52	5.4	6.0	5.9	5.5
Galveston Bay av[b]	4.3 ± 0.4 ($n = 7$)	5.0 ± 0.2 ($n = 7$)	5.3 ± 0.1 ($n = 5$)	5.3 ± 0.2 ($n = 5$)	5.4 ± 0.1 ($n = 5$)

[a] $K_d = Hg_p/[(Hg_d + Hg_c)C_p]$; $K_p = Hg_p/[Hg_dC_p]$; $K_{p+c} = (Hg_p + Hg_c)/[Hg_d(C_p + C_c)]$; $K_c = Hg_c/[Hg_dC_c]$. Hg_p, particulate Hg concentration (cpm/mL). Hg_d, calculated truly dissolved Hg concentration (<1 kDa) (cpm/mL). Hg_c, colloid Hg concentration (1 kDa < Hgc < 0.45 μm) (cpm/mL). C_p, SPM concentration (kg L^{-1}). C_c, colloidal organic matter concentration (kg L^{-1}). [b] After Stordal et al. (*6*).

TABLE 3

Kinetic Rate Constants (k_1 and k_2) and Coagulation Rate Constant (B_t) for Experiments with Varying Particle Concentrations (C_p) and Salinities (S)

experiment	S	C_p (mg L^{-1})	$k_1{}^a$ (h^{-1})	$1/k_1$ (h)	r^2	$k_2{}^a$ (h^{-1})	$1/k_2$ (h)	r^2	B_t (h^{-1})	t_s (h)
particles	0.1	27	0.24	4.2	0.69	4.6e−3	217	1.0	0.07	13.7
particles × 1/2	0.1	10	0.18	5.6	0.41	7.2e−3	139	0.88	0.04	22.7
particles × 2	0.1	42	0.32	3.1	0.87	1.1e−2	95	0.62	0.09	10.7
particles × 4	0.1	82	0.36	2.8	0.87	1.1e−2	94	0.29	0.14	7.1
seawater	24.4	34	0.5	2.0	0.96	5.3e−3	190	0.52		
intermediate salinity	13.6	30	0.29	3.4	0.2	3.6e−3	276	0.1		

[a] Regression between log k_1 (or k_2) with log C_p yield. Log $k_1 = -1.1 + (0.035 \pm 0.05)$ log C_p; $r = 0.98$. Log $k_2 = -2.5 + (0.23 \pm 0.26)$ log C_p; $r = 0.52$.

$$M_c/(M_c + M_p) = \exp(-k_1 t) \qquad (1)$$

where M_c is the concentration of metal associated with colloids (cpm/mL), M_p is the concentration of metal associated with particles (cpm/mL), and k_1 is the rate constant in units of inverse time. The value for k_1 can be determined (from the slope of the line) by plotting $\ln(M_c/(M_c + M_p))$ versus time. Applying this model using data from the Trinity River at a particle concentration of 27 mg/L suggests that there are two distinct reaction processes with different rates (Figure 6). The first region is observed over the course of the first hour and has a rate constant of 0.24 h^{-1} or a characteristic time ($1/k_1$) of 4.2 h (Table 3). A slower rate ($k_2 = 4.61 \times 10^{-3}$ h^{-1}) is observed for time scales of 1−5 days and has a characteristic time ($1/k_2$) of 9 days. Rate constants calculated at several particle concentrations and salinities are given in Table 3.

When plotting the values of k_1 and k_2 as a function of suspended matter (SPM) concentration on a log scale (Figure 7), it becomes quite evident that these rate constants are a power function of SPM ($k = a[\text{SPM}]^b$) with values for b of 0.35 ± 0.05 for the fast process (k_1) and 0.23 ± 0.26 for the slow process (k_2) (Table 3). A value of 0.3 would be expected for Brownian coagulation (see below). Thus, both rates are likely related to two distinct but minor populations of colloids that coagulate with different rates onto the filterable particles. The sum of these two colloidal Hg fractions is ≤10% of the colloidal organic carbon concentration (COC) as determined from separate experiments.

In comparison, the colloidal pumping model, as described by Honeyman and Santschi (11) and based on the work of Farley and Morel (12), allows one to calculate a pseudo-first-order coagulation rate coefficient from

$$B_t = B_b C_p{}^{0.3} + B_{sh} C_p{}^{0.9} \qquad (2)$$

Pseudo-first-order rate constants for coagulation by Brownian motion (B_b) and shear (B_{sh}) can be estimated from parameters in the literature for similar situations. A shear rate constant of 0.1 s^{-1} was estimated from the stirring rate in the beakers; an excess floc density ($\rho_e - \rho_f$) of 0.1 g cm^{-3} was estimated based on previous work (21, 22); and a collision efficiency factor of 0.05 (23) was estimated. For the height of the water column, we used the bottle height of 17 cm. From these parameters, calculated values of B_t range from 1 to 3 day^{-1} (Table 3). Under these circumstances, the characteristic time scales ($t_s = B_t{}^{-1}$) for coagulation/sedimentation range from 7 to 23 h and decrease with increasing particle concentration. These calculated rates using typical parameter values are intermediate between k_1 and k_2 and indicate the correct order
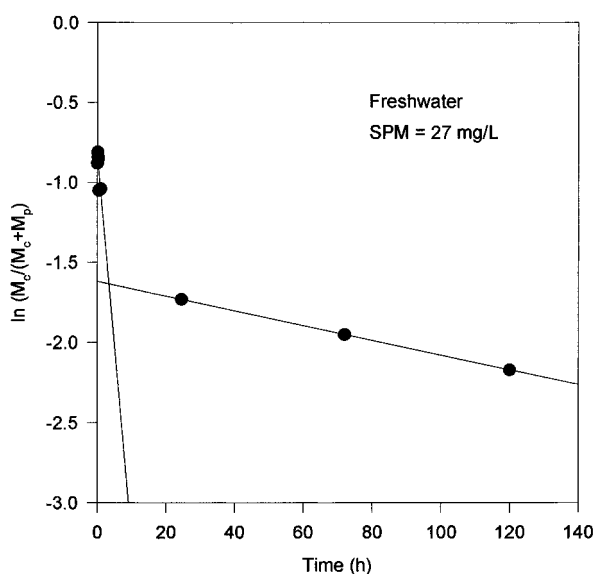

FIGURE 6. Ln ($M_c/(M_c + M_p)$) versus time (h) for the mixing experiment of Trinity River water with SPM (27 mg/L). M_c = colloidal ^{203}Hg (cpm), M_p = particulate ^{203}Hg (cpm).
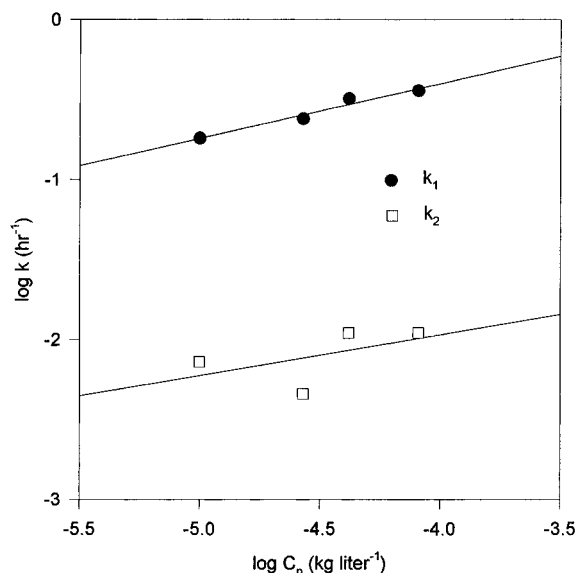

FIGURE 7. Relationship of log k_1 and k_2 with log C_p (or SPM) for the Trinity River samples. Equations for the regression lines are given in Table 3.

of magnitude of hours to days. The parameters chosen are however only approximations to the experimental conditions. Since the results of these calculations are sensitive to the exact choice of parameters which are, however, not

exactly known for these experiments, it is not useful to attempt to exactly simulate the experimental results. However, the simulations support our contention that colloidal forms of Hg can coagulate to larger particles.

Acknowledgments

Literature Cited

(1) Schindler, P. W. *Thalassia Jugoslav.* **1975**, *11*, 101−111.
(2) Li, Y.-H. *Geochim. Cosmochim. Acta* **1981**, *45*, 1659−1664.
(3) Balistrieri, L. S.; Brewer, P. G.; Murray J. W. *Deep-Sea Res.* **1981**, *28*, 101−121.
(4) Bruland, K. W.; Donat, J. R.; Hutchins D. A. *Limnol. Oceanogr.* **1991**, *36*, 1555−1577.
(5) Morel, F. M. M.; Dzombak, D. A.; Price, N. M. In *Ocean Margin Processes in Global Change*; Mantoura, R. F. C., et al., Eds.; Wiley: New York, 1991; pp 165−180.
(6) Stordal, M. C.; Gill, G. A.; Wen, L.-S.; Santschi, P. H. *Limnol. Oceanogr.* **1996**, *41* (1), 52−61.
(7) Wen, L.-S.; Stordal, M. C.; Tang, D.; Gill, G. A.; Santschi, P. H. *Mar. Chem.*, in press.
(8) Wen, L.-S.; Santschi, P. H.; Gill, G. A.; Paternastro, C. *Mar. Chem.*, submitted.
(9) Li, Y.-H.; Burkhardt, L.; Buchholtz, M.; O'Hara, P.; Santschi, P. H. *Geochim. Cosmochim. Acta* **1984**, *48*, 2011−2019.
(10) Nyffeler, U. P.; Li, Y.-H.; Santschi, P. H. *Geochim. Cosmochim. Acta* **1984**, *48*, 1513−1522.
(11) Honeyman, B. D.; Santschi, P. H. *J. Mar. Res.* **1989**, *47*, 951−992.
(12) Farley, K. J.; Morel, F. M. M. *Environ. Sci. Technol.* **1986**, *20*, 187−195.
(13) Li, Y.-H.; Burkhardt L.; Teraoka, H. *Geochim. Cosmochim. Acta* **1984**, *48*, 1879−1884.
(14) Santschi, P. H.; Nyffeler, U. P.; Li, Y.-H.; O'Hara, P. In *Sediments and Water Interactions*; Syl, P. G., Ed.; Springer-Verlag: New York, 1986; Chapter 17.
(15) Niven, S. E. H.; Moore, R. M. In *Radionuclides: A Tool for Oceanography*; Guary, J., et al., Eds.; Elsevier: Amsterdam, 1988; pp 111−20.
(16) Gill, G. A.; Bruland, K. W. *Environ. Sci. Technol.* **1990**, *24*, 1392−1400.
(17) Stordal, M. C.; Gill, G. A. *Water, Air, Soil Pollut.* **1995**, *80*, 725−734.
(18) Buffle, J. *Complexation reactions in aquatic systems: an analytical approach*; Ellis Horwood: Hempstead, U.K., 1990.
(19) Hering, J. G.; Morel, F. M. M. In *Aquatic Chemical Kinetics*; Stumm, W., Ed.; John Wiley & Sons: New York, 1990; pp 145−172.
(20) Jannasch, H. W.; Honeyman, B. D.; Balistrieri, L. S.; Murray, J. W. *Geochim. Cosmochim. Acta* **1988**, *52*, 567−577.
(21) Komer, P. D.; Morse, A. P.; Small, L. F. *Limnol. Oceanogr.* **1981**, *26*, 172−180.
(22) Alldredge, A. L.; Gotschalk, C. *Limnol. Oceanogr.* **1988**, *33*, 339−351.
(23) O'Melia, C. R. In *Aquatic Chemical Kinetics*; Stumm, W., Ed.; John Wiley & Sons: New York, 1990; pp 447−474.